Collective effects of yeast cytoplasmic dynein based microtubule transport

Kunalika Jain, Neha Khetan, and Chaitanya A. Athale*

Electronic Supplementary Information (ESI)

- Supplementary Figures
- Supplementary Tables
- Supplementary Results
- Supplementary Videos

Supplementary Figures

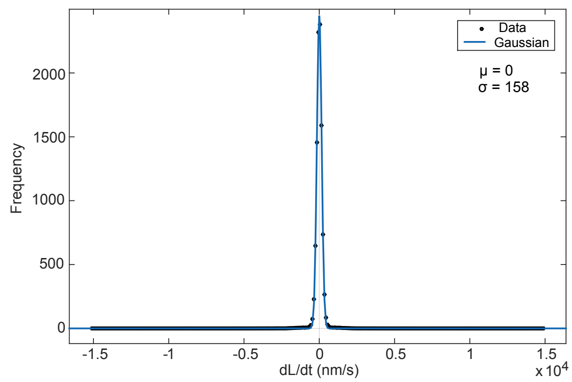

Figure S1: **Estimating changes in MT length during tracking.** MTs were tracked using the nanometer precision filament tracking program, FIESTA [1], and the frequency distribution of the pairwise change in length as a function of time (dL/dt) in nm/s (black circles) was fit to a Gaussian (blue curve) with a mean of 0 nm/s and standard deviation of 158 nm/s.

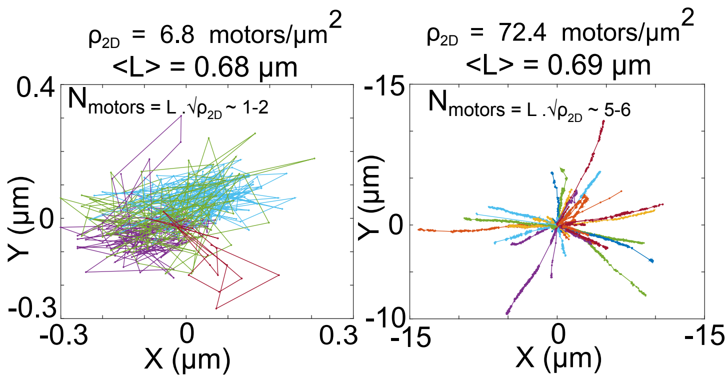

(a)

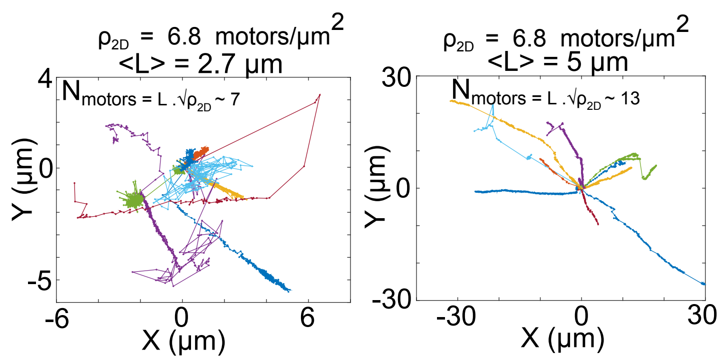

(b)

Figure S2: **Motor number (N) dependence of transport characteristics.** Representative XY trajectories of filaments (plus-tips) represent the effect of increasing motor numbers from (a) $< N >\sim$1 to 2 (n=4) to 5-6 (n=48) for the same length of MTs $\sim$0.7 μm based on motor density (ρ_{2D}). (b) The effect of a change in $< N >$ from 7 (n=8) to 13 (n=17) on XY trajectories is seen for the same motor density, arising from differences in length alone. Colors represent individual trajectories.

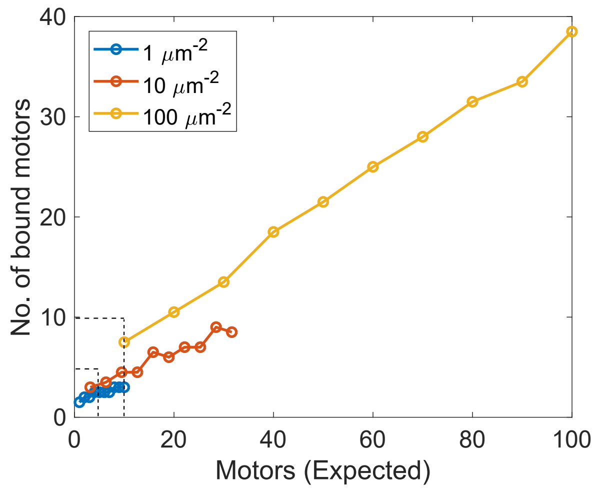

Figure S3: **Number of bound motors per filament from simulations.** The mean number of bound motors per filament (y-axis) is plotted as a function of the expected number of motors encountered (x-axis) from simulations of a yeast dynein gliding assay. The bound motor values are obtained by averaging (time- and filament-average) for 100 MTs over 300 s. Grey dashed lines represent two points on a line with unit slope for 5 and 10 motors on both the axes.

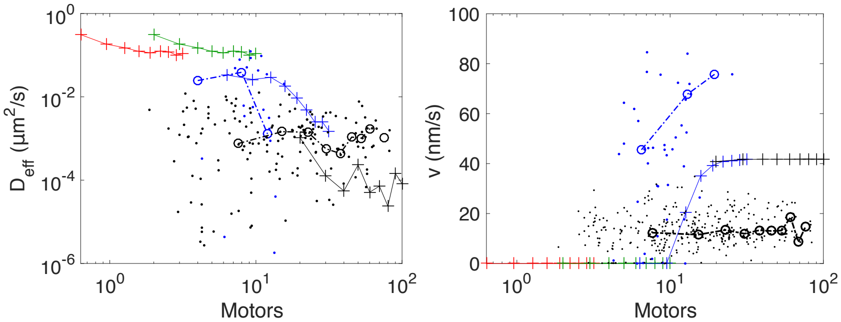

(a) (b)

Figure S4: **Motor number dependence of effective diffusion and transport velocity.** Based on the fits to the diffusion with transport model (a) the effective diffusion coefficient (D_{eff}) and (b) transport velocity (v) of MTs are plotted as a function of the expected number of motors (x-axis). The scatter plot represents experimental values for each filament (dots,), with medians (circles) connected by dashed lines (-.). Blue: low density, black: high density. The median values from simulation (+) are plotted for comparison. Motor density in motors/μm^2 is green: 10^{-1}, red: 10^0, blue: 10^1, black: 10^2.

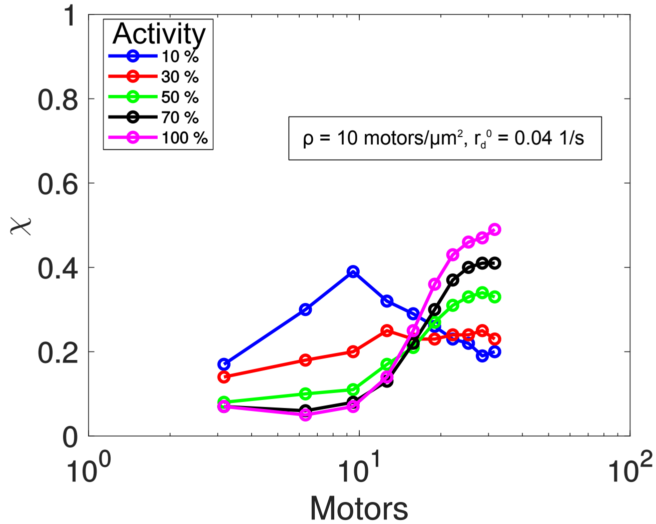

Figure S5: **Effect of motor activity on N-dependence of MT directionality.** Increasing proportion of active motors results in qualitative differences in the profile of directionality with the number of motors (N). Inactive dynein has been modeled as having a zero velocity, i.e. unable to step, while the binding and unbinding kinetics are identical to the 'wild-type' motor, based on the ATP hydrolysis mutant of this dynein[2].

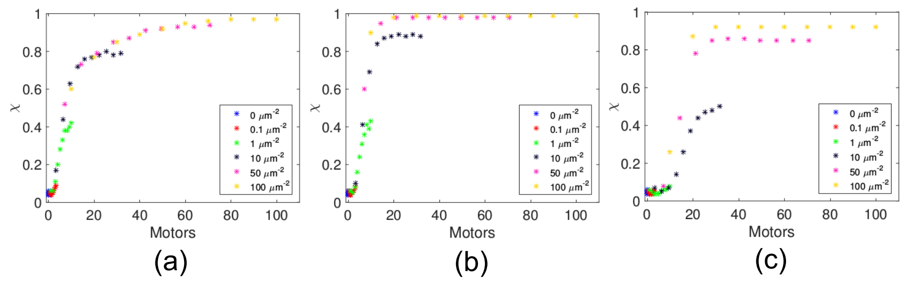

Figure S6: **Simulations of the effect of motor detachment models on directionality.** The change in directionality χ as a function of average motors acting per MT are compared for a range of MT lengths and densities. The detachment models compared are: (a) constant detachment rate of r_d^0 , (b) symmetric detachment rate based on Kramers law $(r_d = r_d^0 \cdot e^{|F_\parallel/F_s|})^{3-5}$ and (c) asymmetric detachment rate that differ in forward and backward directions (Model section 2.2). Colors indicate motor density (ρ_{2D}) and each point corresponds to the mean directionality for a given length ($N_{MT} = 100$). Model parameters in Table 1.

Supplementary Tables

Estimating uncertainty in dynein surface density estimation

		Surface density, ρ_{2D} (μm^{-2})		**Linear density, ρ_{1D} (μm^{-1})**	
Fit, Bounds	**Slope**	Low density	High density	Low density	High density
Fit	112.7	6.8	72.8	2.62	8.53
B1	118.7	6.5	69.2	2.55	8.31
B2	106.7	7.2	77	2.69	8.77

Table S1: **Uncertainty in dynein number estimation.** The table represents the 1D (ρ_{1D}) and 2D (ρ_{2D}) densities of dynein based on the slope of the fit (Fig. 3(b)). Based on a 95% confidence interval, the bounds of the slope B1 and B2 are calculated. Based on these slopes, the corresponding dynein densities are calculated for high- and low-density samples.

Supplementary Results

Simulating the effect of alternative detachment mechanics on MT transport directionality

The model of dynein detachment mechanics is based on previous single-molecule measurements of the minimal truncated *S. cerevisiae* cytoplasmic non-essential dynein[6,7]. We attempted to address whether this asymmetric detachment model is essential to reproduce the length and motor-number dependence of 2D transport directionality. Parameter values of the two alternative models were identical to the more complex asymmetric detachment rate model as described in the model section, and they are:
(a) Constant, load-independent detachment rate

$$r_d = r_d^0 \tag{SEq1}$$

where r_d^0 is the basal detachment rate.
(b) Symmetric load-dependent detachment based on Kramers law[3]:

$$r_d = r_d^0 \cdot e^{|F_\parallel / F_s|} \tag{SEq2}$$

where $F_\parallel$ is the component of the load force parallel to the MT and F_s is the stall force.

We find that while the qualitative shape of the 2D directionality measure increases steeply in all three models tested, the absolute threshold at which directionality increases is higher (∼8-10) when the motor is modeled to detach asymmetrically with load force (Fig. S6). This result appears to point to motor-detachment as a major determinant of the onset of directionally persistent transport, and not density and spacing, which are common to all three motor models.

We speculate, this mechanical property might have evolved to exploit the low density of available dyneins at the yeast bud cortex during ‘search and capture’ of astral MTs, to enable correct orientation of the nucleus by an initial random phase, followed by a sharp transition to directionally persistent motility. Such an idea could be tested in experiments in future.

References

[1] F. Ruhnow, D. Zwicker and S. Diez, *Biophys. J.*, 2011, **100**, 2820–2828.

[2] M. A. DeWitt, A. Y. Chang, P. A. Combs and A. Yildiz, *Science*, 2012, **335**, 221–5.

[3] H. Kramers, *Physica*, 1940, **7**, 284–304.

[4] C. A. Athale, A. Dinarina, F. Nedelec and E. Karsenti, *Phys. Biol.*, 2014, **11**, 016008.

[5] N. Khetan and C. A. Athale, *PLoS Comp. Biol.*, 2016, **12**, e1005102.

[6] F. B. Cleary, M. A. Dewitt, T. Bilyard, Z. M. Htet, V. Belyy, D. D. Chan, A. Y. Chang and A. Yildiz, *Nat Commun*, 2014, **5**, 4587.

[7] M. P. Nicholas, F. Berger, L. Rao, S. Brenner, C. Cho and A. Gennerich, *Proc. Natl. Acad. Sci. U.S.A.*, 2015, **112**, 6371–6376.

Supplementary Videos

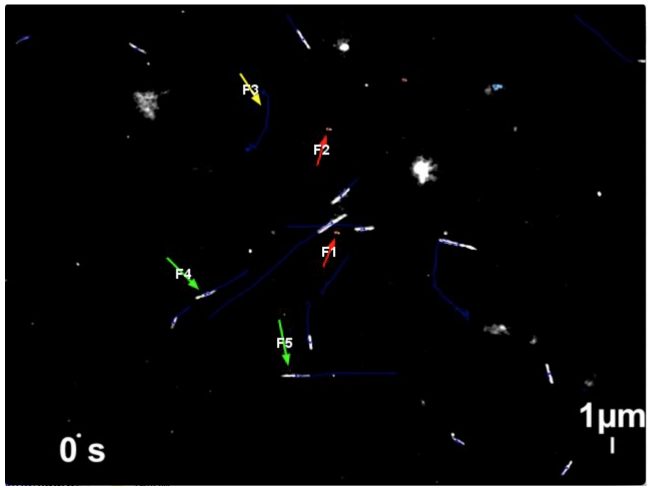

(a)

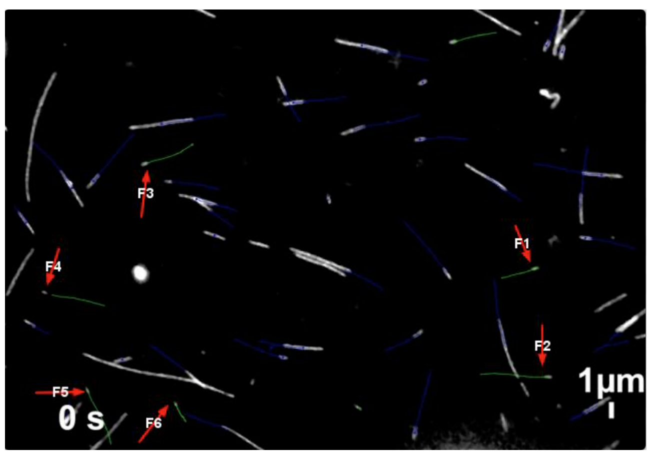

(b)

Video SV1: **Increasing processivity of short filament transport with motor density.** The transport of short filaments with a motor density of (a) 6.8 motors/μm^2 and (b) 72.4 motors/μm^2 is compared between MTs of different lengths. (a) The trajectory of the centroids are overlaid as a guide to the eye (blue). F1,2: L_{MT} ∼0.5 to 0.7 (red), F3: L_{MT} ∼4.7 μm (yellow), F4 and F5: L_{MT} 6.3 and 8 μm (green). (b) Trajectories of short filaments (F1 to F6) are marked green.

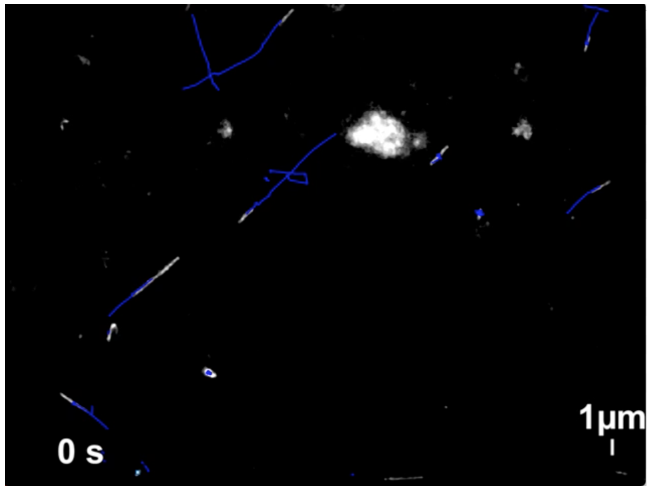

(a)

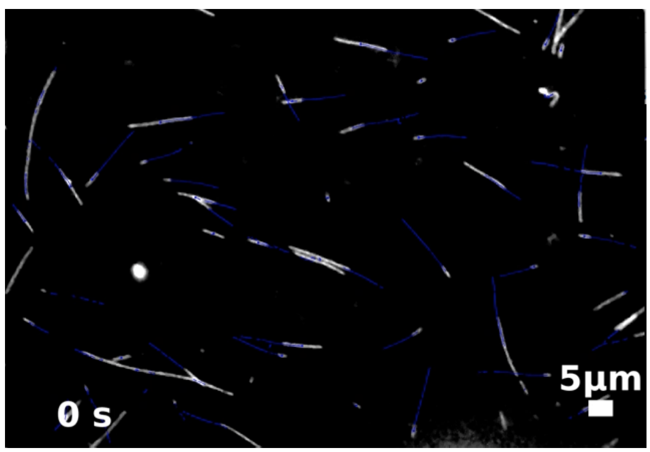

(b)

Video SV2: **Time-lapse movies of MT gliding in experiment.** A time series of MTs gliding in the presence of (a) 6.8 and (b) 72.4 motors/μm^2 dynein were acquired every 1 second. The rhodamine labelled taxol-stabilized MTs (grey) were tracked using FIESTA and tracks are overlaid on the time series (blue lines). The time stamp is in units of seconds and the scale bar is 5 μm.

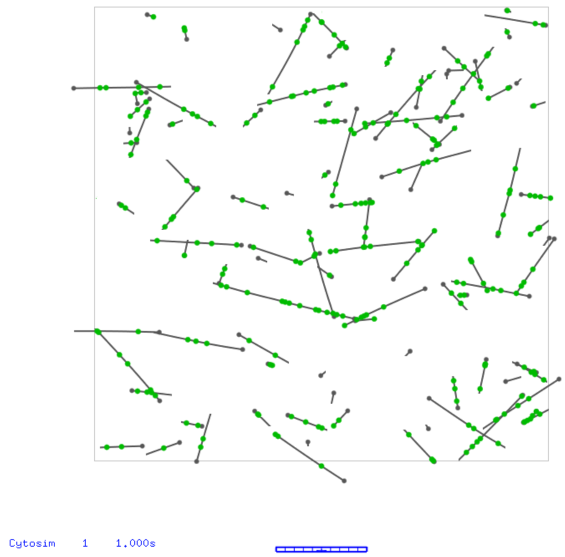

Video SV3: **Simulations of 2D MT transport by dynein**. Simulations of semi-flexible polymers of microtubules as they glide and swivel when attached to motors, and freely diffuse if they are unbound, were performed using Cytosim. The motor density ρ_{2D} is 10 motors/μm^2. Individual MT lengths are constant during the simulation and their lengths are exponentially distributed to reproduce experimental observations. Scale bar 10 μm.

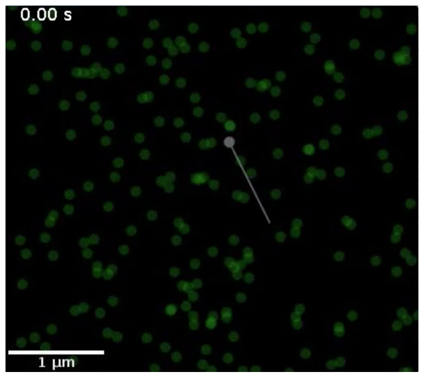

(a)

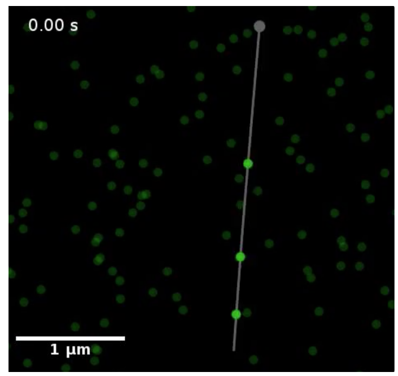

(b)

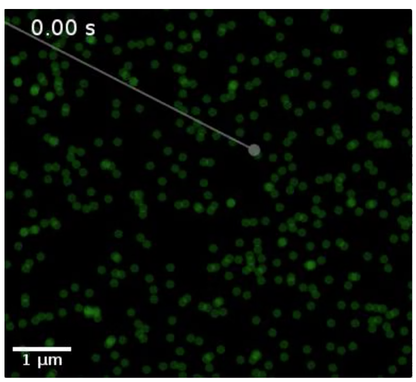

(c)

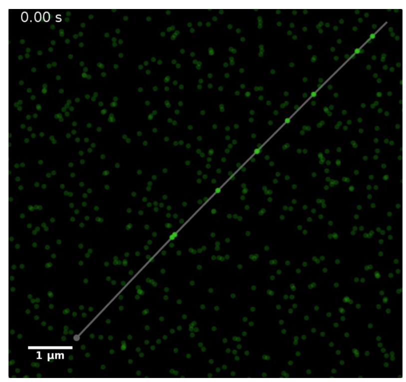

(d)

Video SV4: **'Search' by MTs of increasing MT lengths.** 2D simulated time-series of MTs (grey) with plus-ends marked (closed circle) gliding on dynein motors (bright green: bound, dark green: free) with a density ρ_{2D} of 10 motors/μm^2 for MTs of lengths (a) 1, (a) 3, (a) 5 and (a) 10 μm. Scale bars are 1 μm, but differ in size to accommodate differences in transport distances for the same time.